Validation of an Impact Limiter Crush Prediction Model with Test Data: The Case of the HI-STAR 100 Package

Krishna P. Singh, Alan I. Soler, and Charles W. Bullard
Holtec International
555 Lincoln Drive West
Marlton, NJ 08053, U.S.A.

1.0 Introduction

An impact limiter is an essential appurtenance in a Part 71 transport package. The impact limiter serves to protect the cask contents from excessive deceleration in the event of a mechanical accident. 10CFR71.73 (as do the IAEA regulations) specifies a drop height of 9 meters (30 feet) onto an essentially rigid surface as the design requirement for the impact limiter.

The orientation of the cask relative to the "target" at the instance of the impact, however, is not specified in the regulations. Therefore, the impact limiter must be capable of limiting the cask's deceleration to a prescribed limit regardless of the cask's orientation at impact. In addition to the indeterminacy with respect to the orientation at impact, the impact limiter must be capable of performing its intended function under a wide range of ambient conditions, ranging from –20ºF to 100ºF, and relative humidity from zero to 100%.

2.0 The AL-STAR Impact Limiter

The central purpose of an impact limiter is to limit the maximum deceleration, α_{max} , of a transport package under a postulated drop event to a specified design value. For the regulatory 9-meter hypothetical free drop event, the AL-STAR impact limiter used in the HI-STAR 100 transport package (CoC No. 71-9261) is engineered to limit the maximum rigid body deceleration to 60 times the acceleration due to gravity. The HI-STAR packaging, consisting of the loaded overpack and top and bottom impact limiters (Figure 1) is essentially a cylindrical body with a rigid interior (namely, the overpack) surrounded by a pair of relatively soft crushable structures. The crushable structure (impact limiter) must deform and absorb the kinetic energy of impact without detaching itself from the overpack, disintegrating, or otherwise malfunctioning. Because a falling cylindrical body may theoretically impact the target surface in an infinite number of orientations, the impact limiter must limit decelerations to below 60g's and preserve the limiter-to-overpack connection regardless of the impact orientation. In general, a drop event orientation is defined by the angle of the HI-STAR 100 longitudinal axis, θ, with the impact surface. In this notation, $\theta = 0$ means a side drop and $\theta = 90°$ implies a vertical or end drop scenario. Inasmuch as the top and bottom impact limiter are made of identical crush material, the top or bottom vertical drop events are mathematically and physically equivalent as far as the impact limiter design is concerned. In any orientation, the drop height is measured from the lowest point on the package.

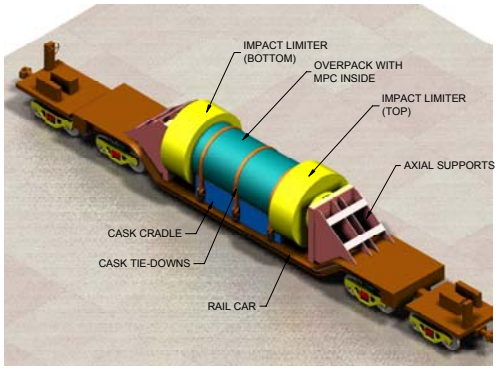

Figure 1: The HI-STAR Transport Package (Personnel Barrier Not Shown)

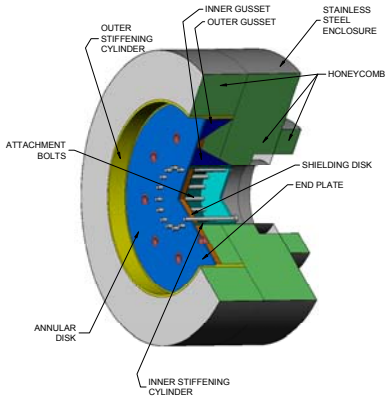

Figure 2: The AL-STAR Impact Limiter

An intermediate value of θ, $\theta = 67.5°$, warrants special mention. At $\theta = 67.5$ degrees, the point of impact is directly below the center of gravity (C.G.) of the HI-STAR 100 package. This drop orientation is traditionally called the C.G.-over-corner (CGOC) configuration. The CGOC orientation is the demarcation line between single and dual impact events. At $90° > \theta > 67.5°$, the leading end of the packaging (denoted as the "primary" impact limiter) is the sole

participant in absorbing the incident kinetic energy. At $\theta < 67.5^\circ$ drop orientations, the initial impact and crush of the leading (primary) impact limiter is followed by the downward rotation of the system with the initial impact surface acting as the pivot, culminating in the impact of the opposite (secondary) impact limiter on the target surface. In the dual impact scenarios, the first and second impact limiter crush events are referred to as the "primary" and "secondary" impacts, respectively. It is reasonable to speculate that for certain values of θ, the secondary impact may be the more severe of the two. The standard design objectives stated in terms of the AL-STAR impact limiter consist of five discrete items, namely:

i. Limit peak deceleration (α_{max}) to 60g's under all potential drop orientations.
ii. Impact limiter must not detach from the cask under a 9-meter drop event under any impact orientation.
iii. The impact limiters must bring the cask body to a complete stop such that the overpack does not come in physical contact with the target surface.
iv. Crush material must be equally effective at -20° and 100° F, with humidity ranging from 0 to 100%.
v. All external surfaces must be corrosion-resistant.

The last two objectives are realized by utilizing aluminum honeycomb (Type 5052) as crush material and stainless steel (Type 304), for the external skin enclosure. As can be seen from the property data compiled in the ASME Code (Section II, Part D, Table Y-1), the essential properties of the constituent material for the honeycomb and the external skin, namely, the yield strength, remain virtually constant in the -20^o F to 100^o F range.

The remaining design objectives, namely, limiting of the maximum rigid body deceleration, α_{max}, to 60g's under a 9-meter drop event, maintaining positive attachment of the AL-STAR impact limiters to the overpack, and preventing contact of the overpack with the unyielding surface, are demonstrated by a combination of theoretical simulations, supported by static and dynamic testing. This was accomplished through a research and development effort that followed six sequential steps:

Step 1: Characterize the honeycomb pressure-deflection relationship.
Step 2: Propose a force (static) vs. crush (F vs. d) model for AL-STAR.
Step 3: Perform 1/8 scale model static compression tests to validate the force-crush model and to establish the adequacy of the AL-STAR backbone structure.
Step 4: Conduct 9-meter quarter-scale model dynamic drop tests in selected limiting drop configurations and obtain test data.
Step 5: Simulate the experimental drop tests with a suitable dynamic crush model and establish that the dynamic model predictions of deceleration, crush and event time duration reasonably match the experimentally measured values.
Step 6: Utilize the experimentally confirmed dynamic crush model to evaluate the effects of tolerances on crush properties and on package weight, and to confirm the adequacy of the full-scale impact limiter design.

It is of crucial importance that the dynamic model benchmarked in Step 5 be of high reliability, since it becomes the analytical model for the accident-event response prediction of the packaging when tolerances on material behavior and package mass are considered (Step 6).

An aluminum honeycomb-based impact limiter design was selected as the energy absorber material for AL-STAR. A pictorial view of AL-STAR is presented in Figure 2. In addition to the crushable honeycomb, the AL-STAR contains two internal cylindrical shells (also denoted as "rings"), which are stiffened with radial gussets. These carbon steel shells are sized to behave as undeformable surfaces during impact events. They are essentially the "backbone" of the impact limiter, lending a predictability to the impact limiter crush behavior and forcing the energy absorption to occur in the honeycomb metal mass.

Another noteworthy aspect of the AL-STAR impact limiter design is the arrangement of uniaxial and cross core (biaxial) honeycombs. Regions of the honeycomb space that experience impact loading in only one direction are equipped with unidirectional honeycomb sectors. The regions where the direction of the impact loads can vary have cross-core (bi-directional) honeycomb material.

3.0 Material Pressure-Crush Relationship

The extent of deflection, Δ, sustained by a honeycomb material when subjected to a uniform pressure, p, is an essential element of information in the impact limiter design. Towards this end, coupon specimens of uniaxial and cross-core honeycomb of various nominal crush strengths and densities were compression-tested by the material manufacturer. The results showed that all honeycomb coupons shared some common load-deflection characteristics [4], namely:

i. The initial pressure-deflection curve resembles an elastic material (pressure roughly proportional to deflection).
ii. Upon reaching a limiting pressure, the material crushes at near constant pressure until the crush reaches approximately 60-70 percent of the initial thickness. The required crush force increases rapidly to achieve small incremental crushing for percent strains beyond approximately 60-70 percent.

Curve fitting of data from all tested coupons indicated that a single mathematical relationship between the applied pressure and compression strain could be developed. The mathematical relationship can provide a reasonable fit for coupons of all crush strengths (crush strength defined as the pressure corresponding to the flat portion of the curve, i.e., it is the constant pressure at which the honeycomb undergoes near-perfect plastic deformation). The pressure, p, for a given strain, ε, is represented by a unique function of the crush pressure, p_c; stated symbolically:

$$p = f(p_c, \varepsilon)$$

The relationship between p and compression strain was used in the subsequent simulation of AL-STAR crush behavior.

4.0 Static Force-Crush Prediction Model

An essential step towards the development of a reliable dynamic model to simulate the impact of a dropped HI-STAR 100 package is to develop a static force-crush model that can subsequently be validated by scale model tests. The force-crush model should reliably duplicate the resistance provided by an impact limiter for a range of crush orientations for the full range of crush depths.

The required force-crush model for AL-STAR is developed using the concept of interpenetration used in contact mechanics [1,2,3]. The inter-penetration theory is explained below using the case of the side drop ($\theta = 0$) as an example (Figure 3a).

The condition existing in all impact limiter crush scenarios is that the relatively soft honeycomb material lies between two “hard” surfaces that are advancing towards each other during the impact. One of these two rigid surfaces is the essentially unyielding target (Rigid Body 1) and the other is the structural backbone of the impact limiter (Rigid Body 2). While the target surface is flat, the backbone structure is cylindrical in profile. When squeezed between the two surfaces, the honeycomb material (at each instant in time) will crush at one or both interface locations. To determine which interface surface will undergo crushing at a given point during the crush event, the concept of interpenetration area is utilized.

In this model, two separate crush scenarios, one assuming that the crush occurs at the external interface (target-to-impact limiter), and the other assuming that the crushing is at the internal interface (structural backbone/overpack-to-impact limiter), are compared at each instant during a simulated compression of the impact limiter. A metal honeycomb impact limiter, in general, may have multiple honeycomb material sections crushing at each interface. For simplicity in explaining the concept of interpenetration, we assume that each of the interfaces is characterized by a uniform distribution of honeycomb having crush pressures p_1 and p_2, respectively. To determine the resistive force developed to crush the impact limiter by a small amount, d, against the external target, the impact limiter is assumed to penetrate the target by the amount “d” without deformation. The resulting area A_1 for the case of side drop, illustrated in Figure 3b, can be computed as an algebraic expression in the amount of approach, d. The pressure-compression relationship for the honeycomb stock at the external interface provides the crush pressure p_1 that develops due to deformation “d”. The total force required for crush “d”, at the external interface, is therefore equal to p_1A_1.

In the second (independent) scenario, the impact limiter external surface is assumed to undergo no movement; rather, the backbone structure (along with the overpack) advances towards the target by an amount d (Figure 3c). Once again, assuming that the cylindrical rigid body moves through an amount "d", the resistance pressure developed in the honeycomb material lying in the path of penetration is available from the appropriate material pressure-compression curve. If the pressure corresponding to the deformation is p_2 and the projected area at the internal interface is A_2, then the total resistive force encountered in realizing an approach equal to "d" between the overpack-backbone assemblage and the target under this latter scenario is p_2A_2. In an actual drop event, at each instant during the event, incremental crush occurs at one of the two interfaces. If $p_1A_1 < p_2A_2$ at a given instant then crushing will occur at the external interface. Likewise, $p_1A_1 > p_2A_2$ will imply that crushing will occur internal to the impact limiter. The smaller of p_1A_1 and $p_2 A_2$ is the required crush force and the corresponding location of crush is where the honeycomb material will compress to realize the approach equal to d.

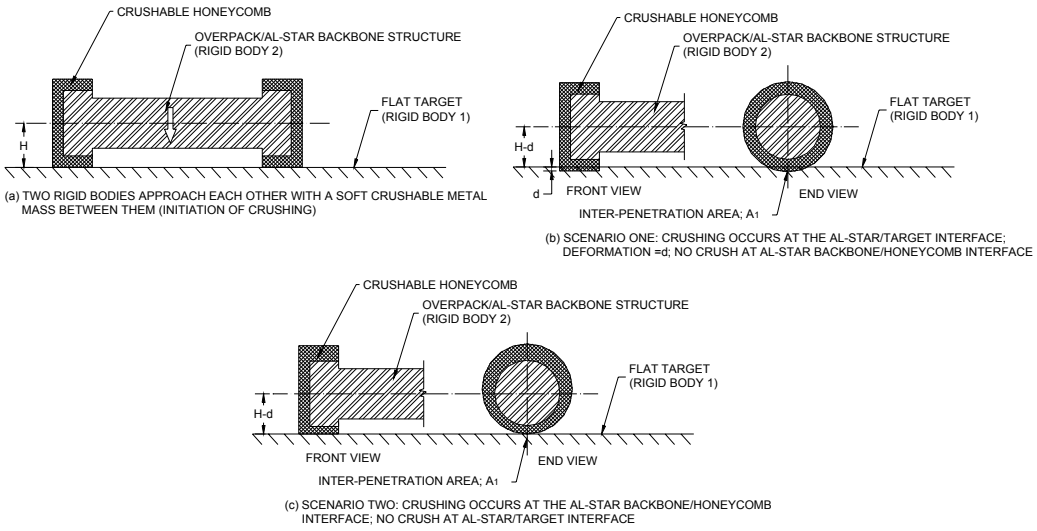

Figure 3: Illustration of the Force-Crush (F-d) Model

This "inequality test" to determine where crushing occurs is performed at every increment of crush during the simulation of the event. The appropriate value of the crush force is used in the equilibrium equations at that instant. The concept of interpenetration at two interfaces has been confirmed by scale testing of the impact limiters; the total crush is observed to be a sum of compression at each of the two interfaces.

To construct a mathematical force-deformation relationship for AL-STAR in any given orientation, the above process is repeated as the crush "d" is increased in small increments starting with the beginning of compression (d = 0). It is quite clear that the development of the force-deflection model (F-d model) for AL-STAR in any orientation is a straightforward analysis in 3-D geometry. The F-d curve for AL-STAR for any given value of θ can be developed where, other than the geometry of the impact limiter, the crush strengths p of the honeycomb materials utilized in the impact limiter are the only other variables.

The force (F) vs. crush (d) relationship developed using the foregoing method is referred to as the F-d model that was subjected to validation by appropriate 1/8 scale model compression tests that are omitted here for brevity, but can be found fully described in reference [6] from which this paper is derived.

5.0 9-Meter Quarter-Scale Model Drop Tests

The series of 1/4 scale model dynamic tests provided physical confirmation of the HI-STAR impact limiter design and the performance of the attachment system. For brevity, only the final series of drop tests are discussed in this paper. In reference [6], whence this paper is derived, all historical drop tests leading up to the final set of tests are described.

In the final series, the 1/4 scale drop tests were performed with four discrete orientations of the cask longitudinal axis with respect to the impact surface, as defined below.

Test A – Vertical Drop (Top End): The cask is dropped such that the deceleration of the cask upon impact is essentially vertical.
Test B: Center of Gravity-Over-Corner (CGOC): For HI-STAR 100, C.G.-over-corner means an orientation wherein the axis of the cask is at 67.5° from the horizontal at the instant of release at the 9-meter height. This test seeks to establish the adequacy of the impact limiter under non-symmetric impact loading.
Test C – Side Drop: The cask is held horizontal with the lowest point on the package 9 meters above the target surface when released for free fall. In this test, both impact limiters participate, and the impact impulse is essentially equally divided between them.
Test D – Slapdown: In this test, the cask axis is held at 15° from the horizontal with the lowest point of the cask assembly at 9 meters from the impact surface. The orientation is such that the top end impact limiter impacts the surface first and the bottom end impact limiter experiences the secondary impact.

Each of the four tests has distinct impact characteristics. For example, in the "side drop" test both impact limiters will strike the target simultaneously; only one impact limiter sustains impact in the "end drop" test. The CGOC test involves a primary impact on one impact limiter at an angle such that the gravity vector is oriented with a line passing through the cask center of gravity and the lowest corner of the limiter. Finally, the slapdown test involves impact at both impact limiters with a very slight time separation. These four tests are deemed to adequately represent the limiting impact scenarios under the hypothetical accident conditions of 10CFR71.73.

A minimum of five calibrated unidirectional accelerometers were installed on the test package for each test. In addition to recording the deceleration during impact, a high-speed camera and a video camera were used to record the test events. The high-speed camera was used to confirm orientation angles just prior to impact and to aid in the evaluation of extent of crush subsequent to the test. The tests were conducted by attaching the 1/4 scale package to a 15-ton mobile crane through appropriate rigging and lifting the package to the required height. An electronically activated guillotine-type cable cutter device was used for releasing the package for free fall.

The results from the drop tests demonstrated that the HI-STAR 100 package meets all test acceptance criteria, namely:

- Appropriately filtered decelerations of less than 60g's (after appropriate scaling to reflect the full-size mass and geometry) for all tested orientations;
- All attachment bolts remained intact, ensuring that the impact limiters do not separate from the cask body through and after the drop event;
- No impact of the cask body on the target surface.

Table 1 provides the peak deceleration data (under the heading "measured") culled from the accelograms for the four drop scenarios after filtering to remove high frequency effects and after scaling up the results from the 1/4-scale data to the full-size packaging.

6.0 Numerical Prediction Model

The numerical prediction model for dynamic drop events utilizes the previously discussed force-crush (F-d) model and incorporates the information into the dynamic equations of equilibrium. Using the procedure discussed previously, the static F-d curves for the AL-STAR impact limiter under the four drop scenarios are readily constructed.

We now discuss the application of the F-d model to the prediction of impact limiter performance in a dynamic drop environment. In symbolic form, we can write the static resistive (crush) force, F, as a function of the crush depth, Δ, where a zero value for Δ, represents an uncrushed condition.

$$F = f(\Delta)$$

In general, the static F-d curve can be expressed as a sum of local crush pressures multiplied by interface areas where the interface areas may be a function of the current crush. That is, the mathematical relation for static compression (which is validated by comparison to static testing) is also expressible in the form

$$f(\Delta) = \sum_i p_i A_i$$

where p_i are the crush pressures of the materials participating in the crush and A_i are the interface areas associated with the different crush strengths. The determination of the areas A_i as a function of crush depth, Δ, has previously been discussed within the context of interpenetration.

The dynamic model for simulating a packaging drop event consists of solving the classical Newtonian equations of motion. In the case of a unidirectional impact such as an end drop (θ=90°), side drop (θ=0), or CGOC drop, the equation of motion simply reduces to:

$$M\frac{d^2\Delta}{dt^2} = \text{Force} + Mg; \text{ where } M = \text{mass of system undergoing deceleration}$$

$d^2\Delta/dt^2$ = second derivative of package movement (which is equal to the impact limiter crush because the target is immovable and rigid).

The resistive "Force" opposes the downward movement and is given by the static force-crush functional relationship (appropriate for the drop orientation) multiplied by a dynamic multiplier z. As noted earlier, there is historical evidence that metal honeycomb crush pressure is a linear function of velocity [4]. Numerical simulations show that an acceptable correlation is achieved if the dynamic multiplier is represented by a linear function of local crush velocity ($d\Delta/dt^2$) Introducing the dynamic multiplier, the dynamic equation of force equilibrium for a case involving only primary impacts becomes

$$M\frac{d^2\Delta}{dt^2} = zF + Mg = zf(\Delta) + Mg$$

The above equation is a second order non-linear differential equation in the time coordinate t, can be solved for the post-contact event using any standard equation solver package. The initial condition is: @ t = 0, Δ = 0, $d\Delta/dt = V_o$ (approach velocity at impact). We note that since the acceleration is an explicit function of both deformation and velocity, maximum acceleration will not, in general, occur at the instant when the velocity of the package is zero.

If the impact event involves both primary and secondary impacts, as is the case for the slapdown event (indeed any event wherein θ<67.5°), then both the mass M and rotational moment of inertia I are involved. The modeling of a dual impact event is only slightly more involved than the single variable modeling of the single impact case discussed above. Figures 4a through 4c illustrate the sequence of events leading to an appropriate mathematical model. Figure 5 provides the appropriate free-body diagrams associated with each portion of the event.

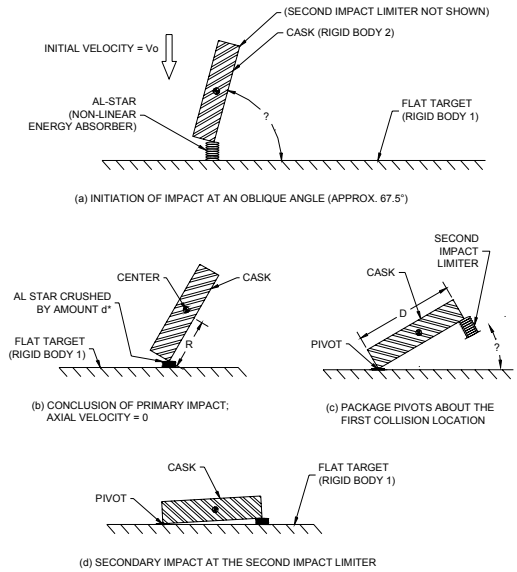

Figure 4: Dynamic Model for a Dual Impact Scenario

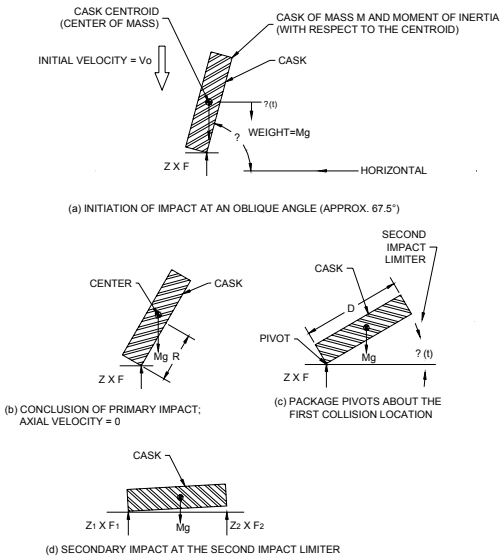

Figure 5: Free-Body Diagram for the Dual Impact Scenario

In the first step, the inertia force of the falling package is resisted by the crush force developed at the primary impact location. While the downward momentum of the package is dissipated by the resistive force, the package also experiences the overturning couple produced by the non-co-linearity of the inertia force (which acts at the centroid) and the resistive force that acts at the primary impact zone (Figure 4a). The dynamic equation of force equilibrium is given above in terms of the downward movement of the package centroid and the resistive force static compression curve, modified by the dynamic factor Z, appropriate to the initial orientation at primary impact. The package decelerates and then begins to overturn, in effect pivoting about the initial point of contact in the primary impact region, gathering angular momentum as the second impact limiter (mounted at the far end) approaches the target surface. Referring to Figure 4b, the dynamic equation ensuring moment equilibrium during the overturning (before the initiation of the secondary impact) Step can be written as

$$I_p \frac{d^2\phi}{dt^2} = -MgR\cos(\phi);\ \text{where}$$

I_p: moment of inertia of the package about the pivot point
ϕ: angular acceleration with respect to the horizontal plane
R: radial distance of the package C.G. with respect to the pivot point.

The initial conditions for this step are: t= 0, $\phi = \theta$, $d\phi/dt = 0$ where t is now redefined at the initiation of rotational motion.

Finally, the secondary impact commences wherein the angular momentum of the package plus any linear momentum not dissipated by the primary impact is dissipated by the crushing of the second impact limiter. During the secondary impact Step, the equation of dynamic moment equilibrium can be written by inspection of Figure 4c:

$$I_p \frac{d^2\phi}{dt^2} = -MgR\cos(\phi) + zf(D\phi)D$$

where $f(D\phi)$ is the static resistive force at the secondary impact location under compression $D\phi$, Z is the current dynamic multiplier appropriate to the secondary impact location, D is the moment arm, and I_p is the moment of inertia of the package about the pivot point. During this step of the motion, the equation of dynamic force equilibrium is modified to reflect dynamic resistive forces from both impact limiters since the entire package may continue to move toward the target surface with both impact limiters providing the dynamic resistive force. Therefore, during the final step of the impact event, the dynamic force equilibrium equation can be written as

$$M\frac{d^2\Delta}{dt^2} = z_1F_1 + z_2F_2 + Mg$$

where z_i and F_i (i=1,2) represent the dynamic multiplier and static compression force appropriate to the primary and secondary impact limiter behavior during the final Step of the event. The dynamic multipliers z_i (i =1,2) reflect the current value of the local crush velocities at each of the limiters.

The above formulation assumes, for simplicity, that the pivot point does not slide during the overturning or secondary impact Steps.

The dynamic simulation model, constructed in the manner of the foregoing, was utilized to simulate all 1/4 scale drop events. In order to develop a high level of confidence, it was decided that the model should be validated at all three levels, namely, a comparison of acceleration, crush, and duration of impact. In other words, to be acceptable, the numerical prediction model must predict α_{max}, maximum crush sustained d_{max}, and the duration of impact, with reasonable accuracy. Since the actual crush d_{max} could be measured, and the duration of impact and α_{max} were available from accelerometer data, comparison between theory and experiment with respect to all three key indicators was possible. Table 1 provides the results in a concise form for all of the one-quarter scale dynamic drop tests.

Note that in the tables, the comparison is made after scaling up the model results to reflect a full-scale package.

Table 1: Comparison Between Test Data and Prediction Model Results

	Deceleration (g's)		Total Crush Depth (inch)			Impact Duration (milli-seconds)	
Case I.D.	Predicted	Measured	Predicted	Measured	Max. Available	Predicted	Measured
A. End Drop	53.0	53.9	11.3	10.6	17.659	38.8	37.2
B. C.G.-Over-Corner	38.7	38.8	12*	9.82*	25.06	51.0	61/45.2
C. Side Drop	43.5	45.7	10.9	12.5	16	38.5	53.1 (averaged value)
D. Slap-Down							
Primary	46.4	49.0	9.50	10.7	16	48.5	44.4
Secondary	59.9	59.0	12.8	13.5	16	35.8	41.2

* For C.G.-Over-Corner, only crush at the external interface is measured.

It is evident from Table 1 that the numerical prediction model is robust in predicting all impact data. Not only are peak values of α_{max} for each test predicted with good agreement, but also the crush depth and impact duration is also reliably simulated.

The agreement between the predictions and measured data in the above correlation effort fosters a high level of confidence in the numerical model to permit sensitivity studies to prognosticate the effect of small changes in the design parameters.

7.0 Closure

The AL-STAR impact limiter design was subjected to a series of static and dynamic tests to validate its functional performance. The 1/8 model static tests conducted under cold and hot, as well as ambient conditions, confirmed that AL-STAR's functional characteristics are independent of the environmental temperature conditions in the range specified in 10CFR71.73. The static tests on the 1/8 scale model (namely, end test and 60° oblique test) were correlated well with the theoretical force-crush model developed by the analytical model based on classical contact mechanics.

A series of 9-meter drop tests were used to define the dynamic factor as a function of velocity approach at impact applicable to the crush material. The dynamic crush model was found to predict the crush depth, the duration of crush and peak deceleration with reasonable accuracy.

Finally, the AL-STAR impact limiter test and qualification program showed that the interpenetration area principle used in the classical non-Hertzian contact mechanics can be successfully implemented to characterize the force-crush relationship of honeycomb impact limiter materials. The test program also demonstrated that, by running an array of drop tests in a variety of collision orientations, a velocity-dependent expression for the dynamic impact factor can be defined. Finally, classical Newtonian equations of motion can be written specific to the mechanics of the impact limiter crush phenomena to characterize the dynamic response of the package with reasonable accuracy. The three indices of impact event, namely, the crush depth, duration of crush, and maximum deceleration, were all predicted with reasonable conservatism in all of the AL-STAR drop tests. AL-STAR crush model thus benchmarked dynamic model can now be used to predict the response of the HI-STAR package in any configuration of impact (θ = 0 to 90°). Insofar as the underpinnings of the theoretical models for static crush and dynamic impact are not honeycomb material or HI-STAR-package specific, they can be utilized to develop impact limiter designs for other packages and crush materials as well.

The central thrust of the work presented in this paper is to provide a tool for designing an impact limiter for a specific application. As such, the methodology is deliberately structured to be adaptable to a wide variety of impact limiter shapes and sizes. If the design of an impact limiter is fully articulated and the object is to predict response under a specific impact configuration, then a finite element solution such as that described in Ludwigsen and Ammerman [7] may be used instead of the design oriented method described in this paper.

8.0 References

[1] Singh, K.P. and Paul, B., "A Method for Solving Non-Hertzian Elastic Contact Problems", Transactions of the ASME, Journal of Applied Mechanics, Vol. 41, Number 2, p. 484-490, June 1974.

[2] Singh, K.P., and Paul, B., "Stress Concentration in Crowned Rollers", Journal of Engineering for Industry, Trans. ASME, Vol. 97, Series B, No. 3, 990-994 (1975).

[3] Singh, K.P., Paul, B., and Woodward, W.S., "Contact Stresses for Multiply-Connected Regions - The Case of Pitted Spheres, Proceedings of the IUTAM Symposium on Contact Stresses, August 1974, Holland, Delft University Press, 264-281, (1976).

[4] J.M. Lewallen and E.A. Ripperger, Energy Dissipating Characteristics of Trussgrid Aluminum Honeycomb, SMRL RM-5, University of Texas Structural Mechanics Research Laboratory, 1962.

[5] Working Model 3.0, Knowledge Revolution, 1995.

[6] HI-STAR 100 Safety Analysis Report, Holtec Report No. HI-951251, USNRC Docket No. 71-9261, Washington, D.C.

[7] Ludwigsen, J.S. and Ammerman, D.J., "Analytical Determination of Package Response to Severe Impacts," Sandia National Laboratories, PATRAM '95.